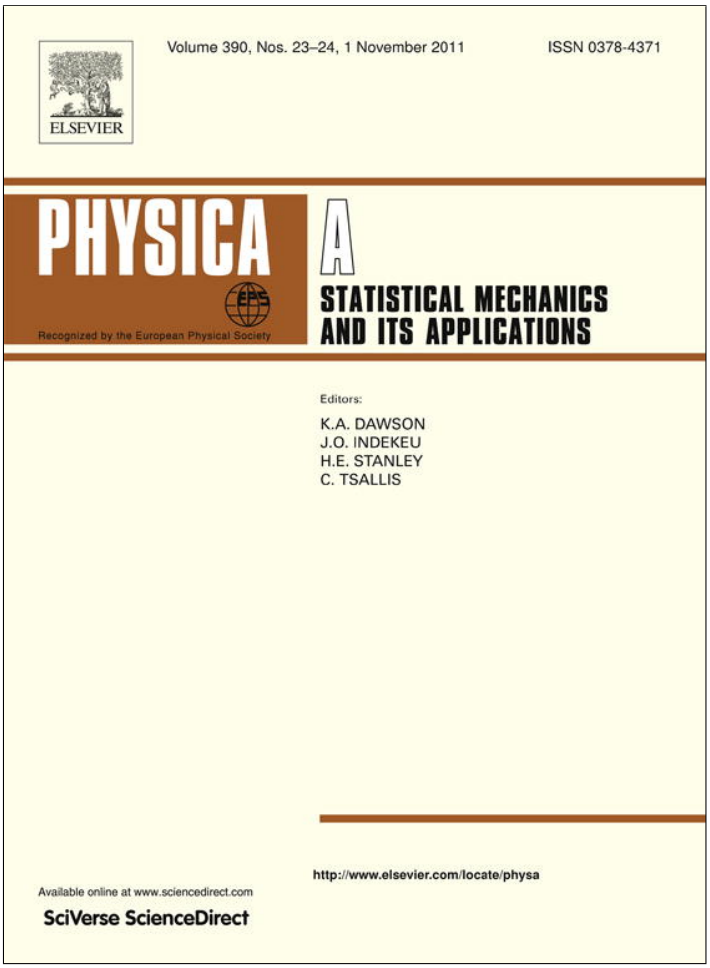

Physica A 390 (2011) 4095–4104

Contents lists available at SciVerse ScienceDirect

Physica A

journal homepage: www.elsevier.com/locate/physa

Critical parameters for measuring angles of stability in natural granular materials

Pablo A. Arias García [a], Rodolfo O. Uñac [a], Ana M. Vidales [a,*], Arcesio Lizcano [b]

[a] INFAP-CONICET, Departamento de Física, Facultad de Ciencias Físico Matemáticas y Naturales, Universidad Nacional de San Luis, Ejército de los Andes 950, D5700HHW, San Luis, Argentina

[b] Departamento de Ingeniería Civil y Ambiental, Universidad de los Andes, Carrera 1. Este No. 19 A-40, Bogotá, Colombia

ARTICLE INFO

Article history:
Received 21 February 2011
Received in revised form 17 May 2011
Available online 26 June 2011

Keywords:
Stability angle
Granular pile

ABSTRACT

In this paper an experimental study of the measurement of stability angles for natural granular piles is presented. The critical dimensions needed for the determination of the angles according to the particle characteristics are established. The material used in the experiments was commonly coarse and fine aggregates used in road construction with a wide range of sizes. Grains were classified by size and characterized through shape factors, apparent density and compacity. The minimum size of the system necessary for measuring the angles of stability was determined depending on the type of experiment to be performed. Results are discussed in terms of the geometry of the different piles and the size of the system.

1. Introduction

Granular materials have drawn a large amount of attention over the last twenty years [1–3]. In particular, the physics underlying the characterization of granular materials involved in the preparation of concrete, pavements or many other civil engineering works is a key part in the development of structural materials. Sand, crushed stone, gravel and several other granular materials involved in those processes are commonly called "aggregates". The properties of these aggregates, as well as their shape (i.e. form and angularity) and texture, substantially affect its overall performance [4–6]. For example, the composition and method of preparation of a standard concrete or of ground prepared for road works, will depend, among other variables, on the type of granular material used, its geometry, origin and hardness. As known, there exist preparation methods that follow empirically well proven standards that guarantee the desired final quality with adequate cost rate. Nevertheless, at the time of initiating a new work or project, materials to be used are generally those that are next to disposition (due to transport costs) and they do not always fulfill the ideal standards. Hence, it is of extreme usefulness to have a basic characterization protocol for the aggregates that will participate in a working project.

Angles of stability are of great importance in determining the response to compression in particulated materials. These angles are related to the internal friction of the material and its resistance to failure [7].

Critical angles have been extensively studied in previous studies [8–12] to characterize the stability of heaps of particles and most of the works were related to the characteristics and dynamics of avalanches [10,13–16]. In general, the stability of a packing of grains can be characterized by the maximum angle of stability θ_M (i.e. the angle at which the grains start to flow) and the angle of repose θ_R (i.e. the angle of the surface right after an avalanche). Besides θ_M and θ_R, there are a set of other angles related to the formation of piles under different manipulation conditions. As could be expected, the stability of the packing is influenced by the number of layers, the packing length and the surrounding humidity [12,17,18].

* Corresponding author. Tel.: +54 2652 436151; fax: +54 2652 436151.
E-mail address: avidales@unsl.edu.ar (A.M. Vidales).

0378-4371/$ – see front matter © 2011 Elsevier B.V. All rights reserved.
doi:10.1016/j.physa.2011.06.055

Table 1
Size classification of the material into five granular sets. FS: Size set. D_p: diameter of largest particle belonging to a given set. Absolute errors for α and β are of the order of 1×10^{-3} and that for Ci is 2×10^{-3}.

FS	D_p (cm)	α	β	Ci
1	0.2	–	–	
2	0.5	0.721	0.711	0.767
3	1.0	0.639	0.719	0.766
4	1.9	0.630	0.742	0.762
5	2.5	0.658	0.750	0.759

Experiments in Ref. [19] have shown that the maximum angle of stability θ_M depends on the initial packing fraction with higher θ_M values for denser packings. Once the avalanche starts, the process evolves, displacing out a well defined quantity of mass and the final free surface always reaches the same angle θ_R. The angle θ_R is independent of θ_M and of the amount of mass displaced: this indicates that θ_R is an intrinsic parameter of the granular medium as generally expected in the literature [20].

Despite all the above, a systematic study to establish the critical dimensions necessary to perform experiments for the measurement of stability angles is lacking for the case of natural aggregates.

The present work focuses on real industrial systems, namely heaps of aggregates that represent the basic raw material for concrete production and road construction. Our objective was to establish a simple methodology for their physical characterization, taking into account that experimental measurement procedures are always conducted on finite assemblies of particles. Aggregates were classified into different granular size sets. We measured aggregate shape parameters, densities, compactness rates, and angles of stability for each size set. The critical lengths of the heaps or packings necessary to measure the corresponding angles of stability were carefully established. Finally, results for the different angles are analyzed, compared and related with the rest of the physical parameters.

2. Physical characterization of the granular material

The materials used in the present study are of current use in road works as well as in the construction of dams and concrete. The raw material was extracted from a quarry next to the city of San Luis in the province of the same name in Argentina. The size classification of the material was performed by sieving the grains in standard sieves. Five granular sets were classified as indicated in Table 1. This classification was inspired by typical grading curves used in civil engineering. The different grain sizes for sets 3, 4 and 5 were obtained by the grinding of natural stone; sets 1 and 2 came directly from natural sources.

The physical characterization of the aggregates consisted in the following steps: (a) classification of the material by size, in five closed grain sized sets; (b) measurement of flatness and elongation rates (α and β, respectively) as a function of the set size; (c) determination of the real density for each set; (d) determination of apparent density (relation mass/volume in a grain packing) for each set; and (e) calculation of compactness.

The shape factors α and β are defined as:

$$\alpha = \frac{T}{W}; \qquad \beta = \frac{W}{L} \tag{1}$$

where T, W and L are the characteristic thickness, width and length of the grains, respectively. If the two shape factors result in being equal to 1, a perfectly cubic (or spherical) shape is assumed for the grain. The smaller the values for these factors, the further from the cubic (or spherical) geometry are the grains.

In the present work, these factors were determined by measuring the three characteristic dimensions, T, W and L, of a representative number of grains taken from each size set. Direct measurement was done by using a digital caliper. It is evident that this method could only be applied to sets 2–5.

An alternative shape factor, the circularity Ci, can be defined as:

$$Ci = \frac{4\pi A_p}{P^2} \tag{2}$$

where A_p is the plane projected area of the particle provided the contribution of gravity will generally ensure that this is the maximal area and P is the length of the perimeter of the projected area. Circularity has the advantage of incorporating a measure of the roughness or surface undulations of the particle [12]. Since we do not have the possibility of digital image processing of the grains, we will calculated Ci approximately by assuming the grain is like a parallelepiped with dimensions T, W and L. With this assumption Eq. (2) can be expressed as:

$$Ci = \frac{\pi LW}{(L+W)^2}. \tag{3}$$

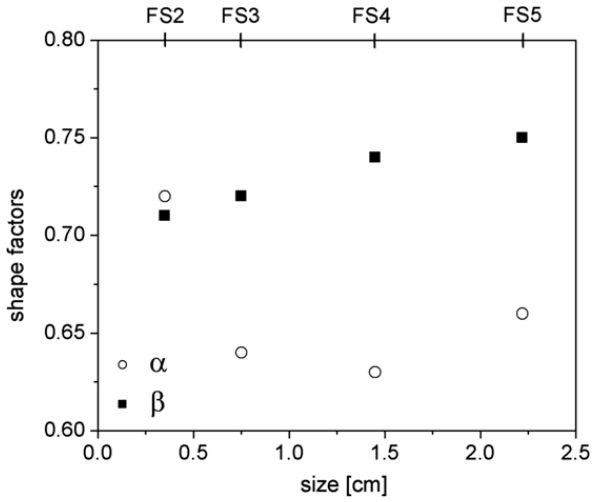

Fig. 1. Results for the flatness and elongation rates (α and β, respectively) as a function of the mean set size. The top axis shows the corresponding set names. Error bars are of the order of symbol sizes.

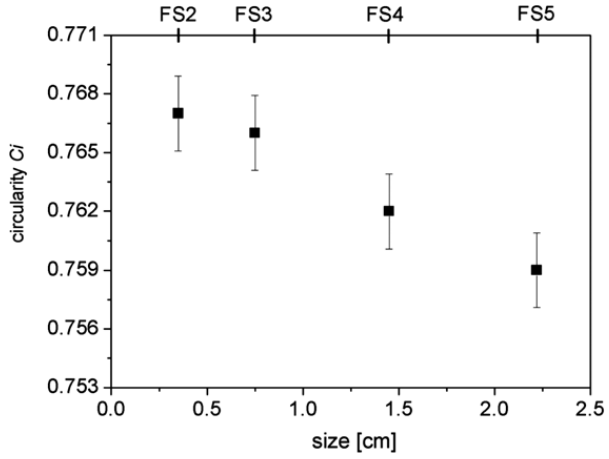

Fig. 2. Circularity of the grains as a function of the mean set size. The top axis shows the corresponding set names. Error bars are indicated.

Besides, it is important to mention that (in our simple assumption that a grain is like a parallelepiped) β is inversely proportional to the ratio between A_p and the area of the smallest inscribed circle into which the grain fits in its entirety, often called the sphericity [12].

Results for the shape factors and the circularity are shown in Table 1 and plotted in Figs. 1 and 2, respectively. As seen in Fig. 1, crushed grains belonging to sets 3–5 present a flattened geometry with respect to set 2, which presents a geometry closer to a spherical grain. For the greatest size sets, the flatness factor is smaller than the elongation one. This feature is related to the flattened geometry presented by crushed grains. The shape factors clearly distinguish the main aspects related to the origin of the aggregates in each set. In general, β shows a tendency to increase with the size of the grains. On the other hand, Fig. 2 shows that *Ci* decreases slightly with size, meaning that the roughness of the grains increases with their size.

An idea about the appearance of the grains can be obtained from Fig. 3 for sets 2–5. The different frames show the four size sets, as indicated by the numbers. Observe the flatness of the grains, while their elongation is less evident.

For the determination of the actual solid density, δ, we employed the standard method that makes use of Archimedes' Principle. For the measurements, ten samples were taken at random from each set. We employed an analytical balance with a 10^{-3} g accuracy. The values for the density δ as a function of the mean grain size (and set) are plotted in Fig. 4. It is observed that values between different sets are comparable, within experimental errors. In other words, the variation of the density is practically negligible and its mean value for the whole sample is taken as (2.6 ± 0.2) g/ml.

The apparent density, δ_a, for the different sets was determined with the help of a container with a well-known volume where the material was poured at a constant height and constant flow rate. The container with the material was weighted using an electronic balance and the apparent density was determined as the ratio between the mass and the volume. The procedure was repeated 15 times to average the results. It is important to note that no vibration was applied to the container at the time of measuring the bulk density in order to reproduce the handling conditions then used in determining the stability angles.

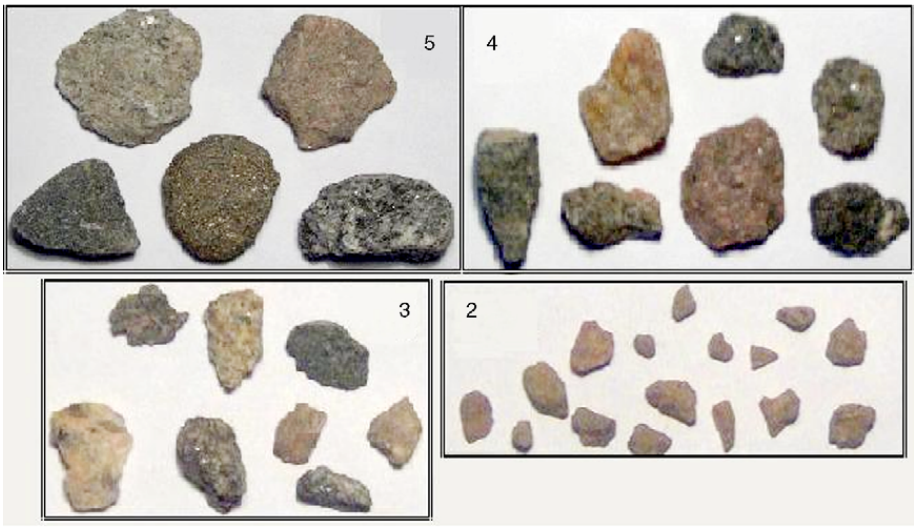

Fig. 3. Appearance of the grains for sets 2–5. The different frames show the four size sets, as indicated by the numbers.

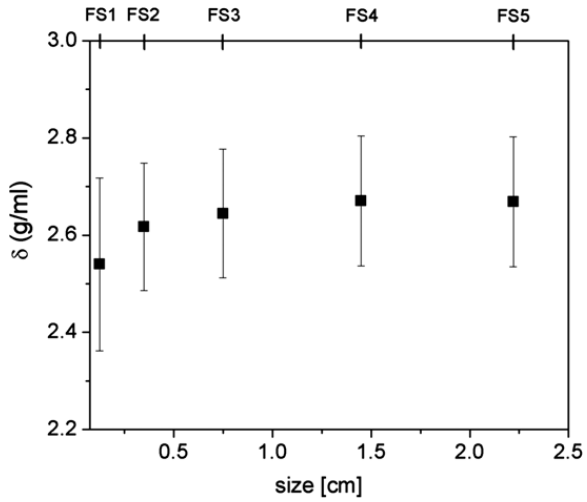

Fig. 4. Values for the density δ as a function of the mean grain size. As before, the top axis indicates the set names. Error bars are indicated.

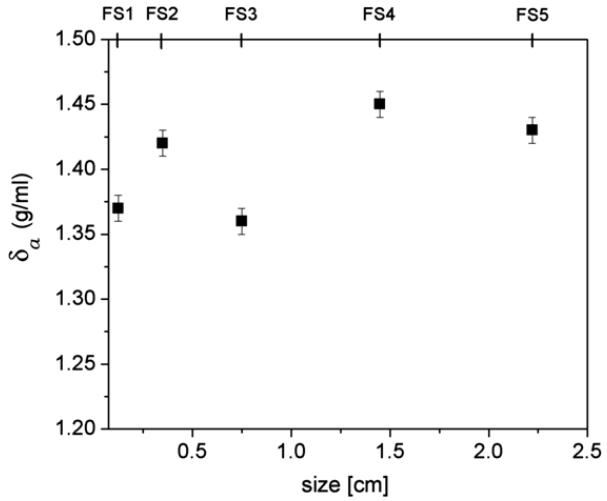

Fig. 5. Values for the apparent density δ_a as a function of the mean grain size. Top axis is like in the previous figure. Error bars are indicated.

In Fig. 5 one can appreciate an increase of δ_a with the size of the grains. In the case of set 3, the grains correspond to the smaller size in a grinding process, i.e., they are the result of an increased fracturing and have a greater angularity than the other sets.

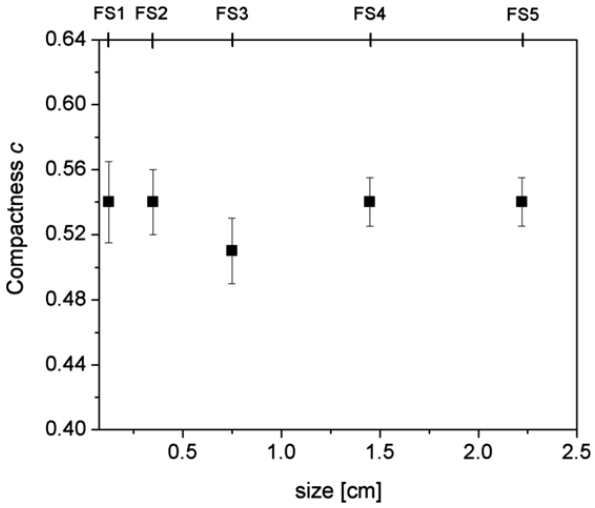

Fig. 6. Compactness c as a function of the mean grain size. Top axis is like in Fig. 2. Error bars are indicated.

In previous studies, we have already observed this trend especially for grains coming from a grinding process [21]. Nevertheless, the interpretation of these data must be done considering the real density of the involved material. For that reason, the compactness c was calculated as the quotient between the volume of grains and the total volume occupied by them, which can be approximated by:

$$c = \frac{\delta_a}{\delta}. \tag{4}$$

c gives an idea on how the grains are arranged in a packing as a function of their size. Different values of c would result in different stability properties for the granular piles.

In Fig. 6 we present the results for the calculation of compactness c as a function of the mean grain size. As observed, small fluctuations are present in c but they are smaller than experimental errors. The different values obtained for δ_a are compensated in some sense by the corresponding values of real density in each set. As a result, compactness does not change notably from set to set. The mean value for all the sets is equal to 0.53, in good agreement with the lowest limit of 0.52 for a gravitational discharge [22]. The values for compactness in Fig. 6 are lower than the typical ones found in previous works for natural aggregates [21]. This is in agreement with the fact that rounded particles, like natural aggregates, have a better compaction capability than irregular ones.

3. Determination of stability angles and critical sizes

3.1. Stability angles

In this section, we define the angles of stability that were measured with different techniques and using a digital goniometer with an accuracy of 0.1°.

As explained before, the stability of a packing of grains can be characterized by the maximum angle of stability θ_M and the angle of repose θ_R. The difference $\Delta = \theta_M - \theta_R$ is typically around 2° or 3° for sands or round grains [9,19]. We also measured this difference in our experiments.

To measure the different angles, and depending on the size of the particles, the experimental set-up included two parallelepiped glass boxes with dimensions (length × height × wide): 40 cm × 30 cm × 25 cm and 20 cm × 30 cm × 14 cm, respectively.

Depending on how an avalanche is induced, a different type of repose angle can be defined. The grains were carefully poured into the box (Fig. 7(a)) up to a height large enough so that the bottom wall had no significant influence on the stability of the pile [13]. Then, a sliding gate was quickly moved upwards so that a certain amount of grains flowed out of the system (Fig. 7(b)), relaxing the surface of the pile to an angle θ_{RT} with respect to the horizontal.

To measure θ_M, θ_R and Δ, the grains were placed in the box as indicated in Fig. 7(c) and then carefully tilted at a constant rotation rate until an avalanche occurred (Fig. 7(d)). The angles were determined as indicated in Fig. 7(d).

In some experiments, local rearrangements of the free surface were observed before the avalanche, in agreement with the observations of Frette et al. [15]. These rearrangements could be easily distinguished from the avalanche itself which represents a "catastrophic" event.

Although the above are the most common, other characteristic angles can be determined to describe the stability of a granular pile. They are the angle of the slope of a conical pile (θ_P) and the angle formed when a drain hole is opened at the base of a granular pile, causing the grains to drain through it, thus forming a crater. For this reason this angle is commonly

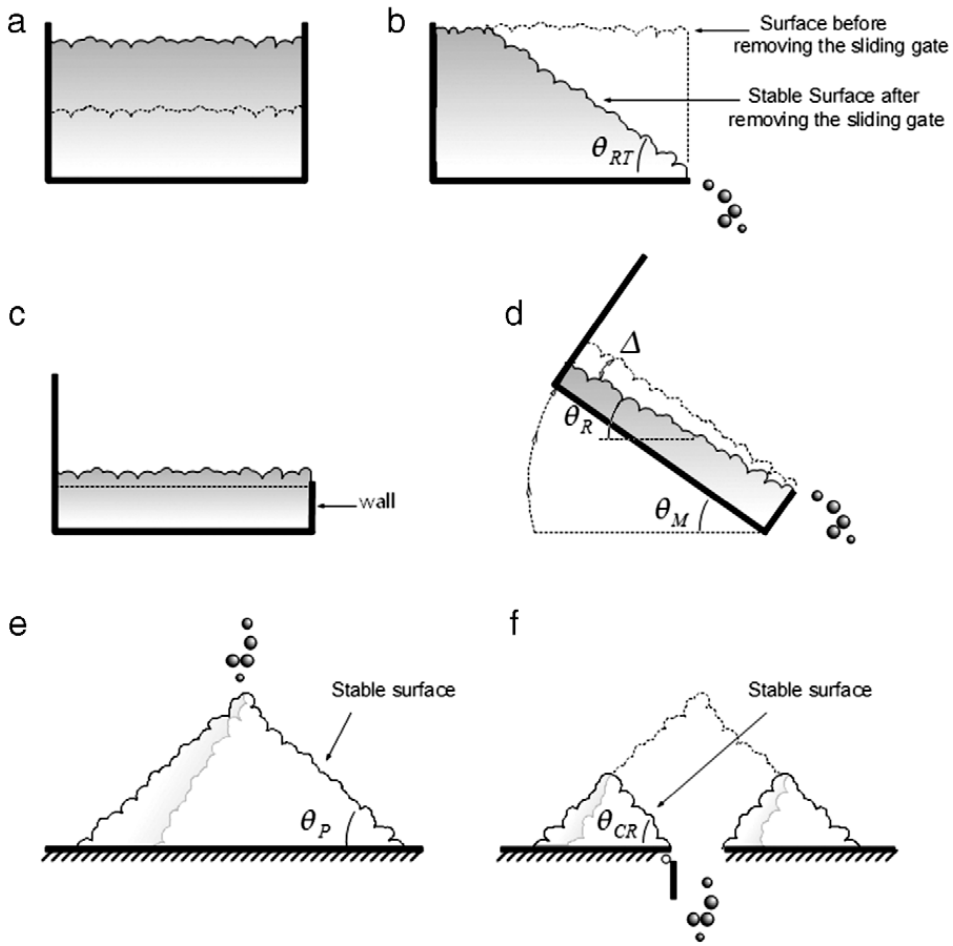

Fig. 7. Sketch indicating the different angles measured in experiments: (a) filling up of the container to measure θ_{RT}; (b) surface after removal of the sliding gate; θ_{RT} is indicated; (c) filling up of the container to measure θ_R and θ_M; (d) inclination of the box at a constant rotation rate until an avalanche occurred, θ_R, θ_M and Δ are indicated; (e) angle for a conical pile, θ_P, and (f) angle for the crater in a conical pile, θ_{CR}.

named the crater angle (θ_{CR}). In Fig. 7, parts (e) and (f) show an outline of the corresponding set-up which consisted of a horizontal table with a central circular hole whose diameter could be varied. A conical pile of granular material was formed on the table by pouring the material at a constant height. Then, the hole was suddenly opened and the grains drained through it. Angles θ_{CR} and θ_P were determined by averaging over 8 measurements performed on different radial directions on the crater and on the slope of the pile, respectively.

Experiments were performed at a low relative humidity, so that capillary and electrostatic effects were negligible.

3.2. Critical sizes

Macroscopic features of a granular pile (or packing) can be clearly observed when the system is large enough. For a small pile, the observed features are the result of local effects, i.e., effects related with the neighboring contacts and the edges.

In the present experiments we assumed the existence of a critical size for the pile to define the macro level; thus, the size of the system must be equal to or greater than the critical size.

The critical size defines the corresponding critical length, L_C, associated with the system property to be measured, i.e., in the present case, the length of the slope of the pile. In what follows, the critical dimension was determined according to each type of experiment and it was such that the slope could be measured experimentally. After numerous tests, it was found that the average slope of the pile was practically constant when measured over a length greater than or equal to 10 times the average particle size, i.e., $L_{C1} = 10D_p$. The critical length was calculated for all stability tests and for each set.

For the determination of Δ, an additional criterion was taken into account in calculating the critical length. Besides the identification of the slope, it is necessary to differentiate θ_M from θ_R. If the slope is not long enough, it may not be possible to distinguish one angle from the other. The length of the slope should be long enough to hold at least one grain as a difference with the slope after the avalanche. This gives the following relationship for the critical length:

$$L_{C2} \geq \frac{180^\circ D_p}{\Delta\pi}. \tag{5}$$

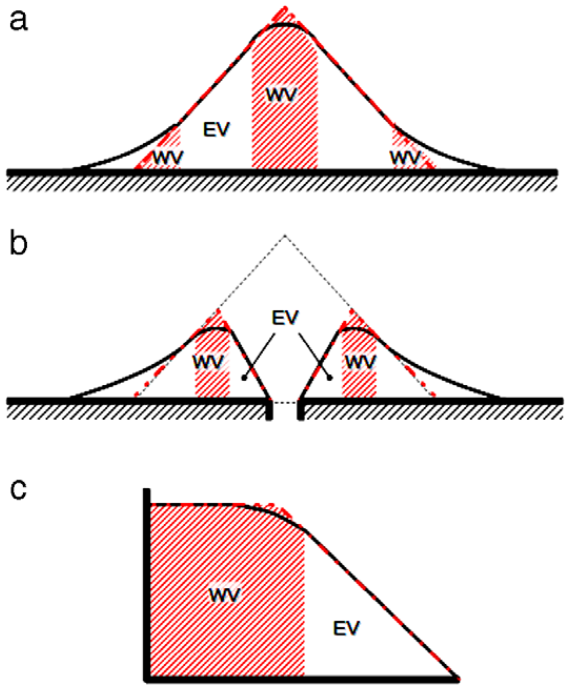

Fig. 8. Sketches for realistic piles where the waste volume (WV) and the effective volume (EV) are indicated for each case: (a) typical pile; (b) pile with a crater; (c) packing of grains after an avalanche.

Table 2
Minimum sizes and weights appropriate to form a pile. FS: size set. D_p: diameter of largest particle belonging to a given set. *BP*: pile base diameter. *HP*: pile height; *WP*: weight of the pile.

FS	D_p (cm)	*BP* (cm)	*HP* (cm)	*WP* (kg)
1	0.2	12	5	1
2	0.5	26	11	3
3	1.0	50	22	20
4	1.9	88	43	127
5	2.5	114	56	273

For a typical value of $\Delta = 2.5^\circ$, this relation gives $L_{C2} \geq 23D_p$. This length is measured along the length of the box. This criterion is more strict than the criterion of 10 particles for L_{C1}.

3.3. Waste and effective volumes, critical sizes and experimental limitations

Fig. 8 shows the corresponding sketches for more realistic piles where it is evident that the length of the slope is not fully usable. This means the presence of zones where no measurements are possible and we call them the "waste volume" (WV). The remaining volume is called the "effective volume" (EV). The length of the slope of this EV must satisfy the calculated critical lengths. Fig. 8 also illustrates and compares the real and ideal profiles involved in the measurements.

The estimation of the critical lengths L_{C1} and L_{C2} for the different packings is straightforward from the values of D_p. Table 2 summarizes the minimum sizes and weights for the different packings. The same pile was used to measure both θ_P and θ_{CR}. If the pile fulfills the critical length for measuring θ_{CR}, then it also does so for θ_P.

The same glass box was used for both Δ and θ_{RT} determinations. The requirement for the former ($L_{C2} = 23D_p$) is more demanding than the one for θ_{RT} ($L_{C1} = 10D_p$); therefore, if it is true for Δ then it holds for θ_{RT}.

As discussed above, a special table was used to build the piles and form a crater. The table dimensions were 99.6 cm × 92.2 cm. The table size limits the maximum size for a pile. Besides, the weight of the material also played an important role to be considered to avoid any bending or deterioration of the table. Measurement of θ_P had no problems in meeting the critical length. On the other hand, for the case of θ_{CR}, the size of the piles built for set 5 was slightly below the critical size.

For the same sets 4 and 5, the size of the greater box was not enough for the determination of Δ with the fulfillment of the requirement in Eq. (5). However, the box size was sufficient to run the test successfully for θ_{RT} in all cases.

The smaller glass box was used for the determination of the angles for sets 1 and 2.

Table 3 summarizes the tests for each set and shows those who have not met the critical length.

Table 3
Verification of the critical lengths (L_{C1} or L_{C2}) for the different sets and angles.

FS	θ_P	θ_{CR}	Δ	θ_{RT}
1	√	√	√	√
2	√	√	√	√
3	√	√	√	√
4	√	√	×	√
5	√	×	×	√

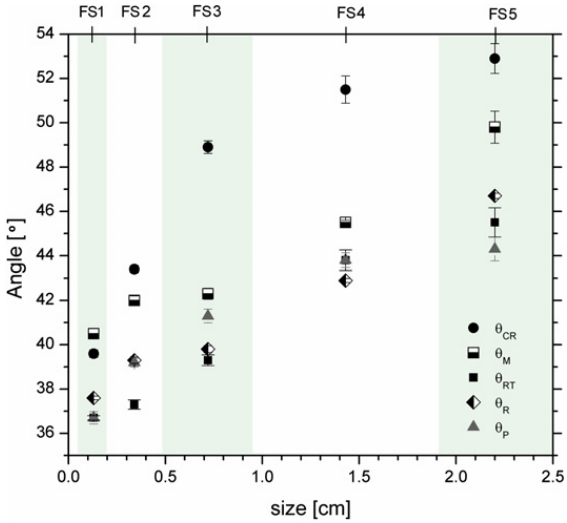

Fig. 9. Stability angles as a function of the mean size of the particles in each set. The top axis shows the set names and the width of the sets is indicated, alternately, in gray and white.

4. Results and discussion on the stability angles

All the stability angles were measured for all sets. Experiments where the critical length was not met were also performed. The angles as a function of the sets size are plotted in Fig. 9. There are a total of five characteristic angles for each set. The value of θ_{CR} is the maximum for all the sets, except for FS $= 1$. The values for θ_{RT} are close below those for θ_R for all sets, except for FS $= 4$.

As expected, the results show that θ_P values are always less than those corresponding to θ_M and fluctuated around the repose angles θ_{RT} and θ_R. It should be noted that two factors play a role in determining θ_P: on the one hand, the stability state of the pile (whether or not near to an avalanche event) and, on the other hand, the convexity of the surface of the pile, which is greater than for the case of θ_R or θ_{RT}.

In general, all critical angles increase with the size of the grains. This is a not so obvious result and should be analyzed taking into account a number of factors. In the first place, it is important to recall that there exists a general conclusion that increasing particle size will decrease the angle of repose. This conclusion is based on experimental and numerical simulations with well controlled parameters and grain geometries, usually using monosized spheres [23–26].

Let us analyze the different factors involved in our present case. On the one hand, the shape factors, particularly β, show a tendency to increase with the size of the grains (Fig. 1) while circularity tends to decrease. At this stage it is interesting to correlate the values of the angles with those for β and *Ci*, as shown in Figs. 10 and 11. It is evident from Fig. 10 that larger stability angles are correlated with a larger β factor; this means that less spherical particles will have greater stability angles. On the other hand, Fig. 11 shows that the increment in the shape factor *Ci* (related to a decrease of the roughness) gives smaller angles of stability. These results are qualitatively consistent with experiments and simulations studying the influence of the surface roughness on the angle of repose of particles in circular rotating tumblers [27].

On the other hand, compactness is practically independent of the grain size (see Fig. 6). This feature reflects the fact that the size distribution for each set behaves as if it were practically a monosize distribution of dry grains, given that cohesive forces or humidity are not present. The characteristics of the size distributions for each set are shown in Table 4. Thus, compactness practically does not change from set to set and will not result in a crucial factor in our present results [11,12].

Finally, note that Δ is practically constant in all the results, even for those cases where the critical conditions were not fulfilled. Its mean value was $(2.8 \pm 0.4)^\circ$.

5. Conclusions

A simple method to characterize aggregates used in civil engineering work is presented. The critical dimensions needed for the determination of the angles according to the particle features are established in detail.

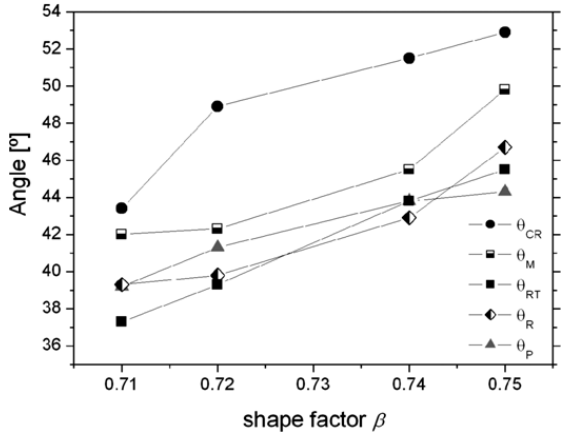

Fig. 10. Correlation between the values of the stability angles and those for the shape factor β.

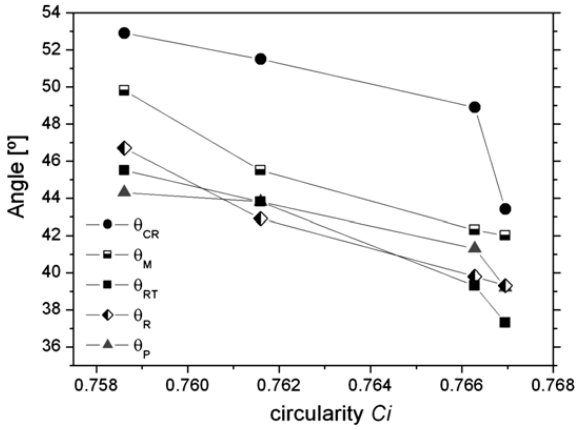

Fig. 11. Correlation between the values of the stability angles and those for the circularity, *Ci*.

Table 4
Relative width (*width*/*mean radius*) of the size distributions and the quotient *r* between the smallest particle size over the largest one for each set FS.

FS	*Width* (cm)	*Mean radius* (cm)	*Width/mean radius*	*r*
1	0.15	0.125	1.2	0.25
2	0.3	0.35	0.85	0.4
3	0.5	0.75	0.66	0.5
4	0.9	1.45	0.69	1.9
5	0.5	2.22	0.22	1.31

The shape factors (the simplest ones chosen for this purpose) clearly distinguish the main aspects related to the origin of each set. In general, they show a tendency to increase with the size of the grains. Compactness does not change notably from set to set and is in good agreement with the lowest limit for a gravitational discharge.

All critical angles increased with the size of the grains. Their values for the different experiments are strongly related with the convexity of the surface of the piles (or packings) involved in the measurements.

Given the results presented above, we conclude that the effect of roughness and shape factors are more important to stabilize the piles than the effect of grain size, which usually diminishes stability angles. For this reason, we expect that in this kind of natural materials the increasing angles will be mainly related to the internal friction and rolling resistance between grains. As a result, stability angles constitute an indirect measurement of the internal friction and resistance of grains and, in this sense, this methodology would serve as a basis for studying internal friction parameters involved in uniaxial and triaxial compression tests, provided the critical lengths discussed here are fulfilled.

Acknowledgments

This work was supported by CONICET (Argentina) through Grant PIP No. 1022 and by the Secretary of Science and Technology of Universidad Nacional de San Luis.

References

[1] H.M. Jaeger, S.R. Nagel, R.P. Behringer, Granular solids, liquids and gases, Rev. Modern Phys. 68 (1996) 1259–1273.
[2] J. Duran, Sables, Poudres et Grains, Eyrolles, Paris, 1997.
[3] H. Hinrichsen, D.E. Wolf (Eds.), The Physics of Granular Media, Wiley VCH, Germany, 2004.
[4] F. de Larrard, A. Belloc, The influence of aggregate on the compressive strength of normal and high-strength concrete, ACI Mater. J. 94 (1997) 417–426.
[5] M. Hunger, H.J.H. Brouwers, Flow analysis of water–powder mixtures: application to specific surface area and shape factor, Cem. Concr. Compos. 31 (2009) 39–59.
[6] A. Kılıç, C.D. Atis, A. Teymen, O. Karahan, F. Ozcan, C. Bilim, M. Ozdemir, The influence of aggregate type on the strength and abrasion resistance of high strength concrete, Cem. Concr. Compos. 30 (2008) 290–296.
[7] I. Herle, G. Gudehus, Determination of parameters of a hypoplastic constitutive model from properties of grain assemblies, Mech. Cohes.-Frict. Mater. 4 (1999) 461–486.
[8] F.C. Franklin, L.N. Johanson, Flow of granular material through a circular orifice, Chem. Eng. Sci. 4 (1955) 119–129.
[9] S.R. Nagel, Instabilities in a sandpile, Rev. Modern Phys. 64 (1992) 321–325.
[10] J. Lee, H.J. Herrmann, Angle of repose and angle of marginal stability: molecular dynamics of granular particles, J. Phys. A 26 (1993) 373–383.
[11] A.M. Vidales, I. Ippolito, O.A. Benegas, F. Aguirre, O.C. Nocera, M.R. Baudino, Granular components of cement: influence of mixture composition, Powder Technol. 163 (2006) 196–201.
[12] D.A. Robinson, S.P. Friedman, Observations of the effects of particle shape and particle size distribution on avalanching of granular media, Physica A 311 (2002) 97–110 and references there in.
[13] F. Cantelaube, D. Bideau, Radial segregation in a 2D drum: an experimental analysis, Europhys. Lett. 30 (1995) 133–138.
[14] M.A. Aguirre, N. Nerone, A. Calvo, I. Ippolito, D. Bideau, Influence of the number of layers on the equilibrium of a granular packing, Phys. Rev. E 62 (2000) 738–743.
[15] V. Frette, K. Christensen, A. Malthe-Sørenssen, J. Feder, T. Jossang, P. Meakin, Avalanche dynamics in a pile of rice, Nature 379 (1996) 49–52.
[16] N. Nerone, M.A. Aguirre, A. Calvo, D. Bideau, I. Ippolito, Instabilities in slowly driven granular packing, Phys. Rev. E 67 (2003) 011302.
[17] N.A. Pohlman, B.L. Severson, J.M. Ottino, R.M. Lueptow, Surface roughness effects in granular matter: influence on angle of repose and the absence of segregation, Phys. Rev. E 73 (2006) 031304.
[18] R. Albert, I. Albert, D. Hornbaker, P. Schiffer, A.-L. Barabasi, Maximum angle of stability in wet and dry spherical granular media, Phys. Rev. E 56 (1997) R6271–R6274.
[19] M.A. Aguirre, N. Nerone, I. Ippolito, A. Calvo, D. Bideau, Granular packing: influence of different parameters on its stability, Granul. Matter 3 (2001) 75–77.
[20] P. Evesque, Analysis of the statistics of sandpile avalanches using soil-mechanics results and concepts, Phys. Rev. A 43 (1991) 2720–2740.
[21] O.C. Nocera, M.E. Médici, O.A. Benegas, P.A. Arias García, R.O. Uñac, A.M. Vidales, Caracterización de áridos para ensayos de resistencia, in: J. Fontana Piatti (Ed.), Los Áridos como Factor de Desarrollo 1, Mar del Plata, Argentina, 2008, pp. 263–269.
[22] I. Zuriguel, A. Garcimartín, D. Maza, L.A. Pugnaloni, J.M. Pastor, Jamming during the discharge of granular matter from a silo, Phys. Rev. E 71 (2005) 051303.
[23] Y.C. Zhou, B.H. Xu, A.B. Yu, P. Zulli, An experimental and numerical study of the angle of repose of coarse spheres, Powder Technol. 125 (2002) 45–54.
[24] A. Burkalow, Angle of repose and angle of sliding friction: an experimental study, Bull. Geol. Soc. Am. 56 (1945) 669–707.
[25] J. Carstensen, P-C. Chan, Relation between particle size and repose angles of powders, Powder Technol. 15 (1976) 129–141.
[26] M. Carrigy, Experiments on the angles of repose of granular materials, Sedimentology 14 (1970) 147–158.
[27] N.A. Pohlman, B.L. Severson, J.M. Ottino, R.M. Lueptow, Surface roughness effects in granular matter: influence on angle of repose and the absence of segregation, Phys. Rev. E 73 (2006) 031304.